A Novel Polyurethane Foam Dressing with Phytochemical Gel for Promoting Diabetic Wound Repair

*Rahul R Padalkar, Ashwini R Madgulkar, Siddharth V. Dumbre, Neha A. Bhandare, Siddhi Joshi, Tanisha Kasbe, Anvi Netragaonkar

[a]AISSMS College of Pharmacy, Kennedy Road, near RTO, Shivaji Nagar, Pune, India 411001

***Corresponding Author**
Dr. Rahul Padalkar

AISSMS College of Pharmacy, Kennedy Road, near RTO, Shivaji Nagar, Pune, India 411001
Phone no. +91-7276720159

Abstract:
Diabetic wounds represent a significant global health challenge, with rising incidence and complex healing requirements. This study aimed to develop an advanced foam dressing integrated with a wound healing gel containing boswellic acid, quercetin, and aloe vera to enhance diabetic wound repair. The gel was formulated and subjected to comprehensive in vitro, ex vivo, and in vivo evaluations to determine its efficacy. In vitro and ex vivo tests demonstrated potent antioxidant and antibacterial properties against *Pseudomonas aeruginosa*, *Bacillus subtilis*, *Bacillus cereus*, *Bacillus coagulans*, *Escherichia coli*, and *Staphylococcus aureus*. In vivo wound healing was assessed using an excision wound model in Wistar rats. Results revealed wound closure rates of 37% in the normal control group and 13.6% in the diabetic control group, while the test formulation achieved a remarkable 98% wound closure, significantly outperforming the standard formulation's 28.4% closure. These findings highlight the potential of the developed foam dressing as an effective therapeutic option for diabetic wound management.

Keywords: Wound, Diabetic wound dressing, Boswellia extract, quercetin, aloe vera.

1. Introduction

A wound is defined as a disruption in the integrity of the skin or other bodily tissues resulting from physical trauma or pathological conditions. Characterized by lesions such as lacerations, contusions, or hematomas, wounds represent a breach in tissue continuity due to external forces or disease processes. Diabetic wounds, a prevalent complication of diabetes mellitus, are particularly significant, predominantly affecting the lower extremities, especially the feet. These wounds exhibit delayed healing and heightened susceptibility to infections compared to non-diabetic wounds, posing substantial clinical challenges. Chronic wounds in diabetic patients arise from impaired wound healing mechanisms, driven by factors such as hyperglycaemia, neuropathy, and compromised immune responses. This impaired healing process results in prolonged recovery periods, increased risk of complications, and significant burdens on both patients and healthcare systems. Consequently, there is an urgent need for research to elucidate molecular mechanisms underlying delayed wound healing in diabetes and to develop targeted therapeutic strategies to enhance tissue repair and regeneration (1).

Diabetic wounds present significant therapeutic challenges due to multiple physiological impairments distinct from those observed in non-diabetic wounds. A primary factor contributing to delayed healing is impaired vascular function, wherein chronic hyperglycaemia induces endothelial dysfunction and microvascular damage, leading to reduced perfusion and inadequate delivery of oxygen and nutrients to the wound site. Additionally, diabetic neuropathy, resulting from prolonged hyperglycaemia, compromises sensory and autonomic nerve function, further hindering the wound healing process by diminishing pain perception and impairing tissue repair signalling. Elevated blood glucose levels also impair immune responses, reducing the body's capacity to combat infections, thereby increasing the risk of wound complications. Inadequate wound care in diabetic patients frequently results in the progression of wounds to severe infections, characterized by deep tissue necrosis and potential osteomyelitis, where infection extends to the bone. Such advanced infections are challenging to eradicate, often necessitating amputation to halt systemic spread and preserve patient survival. These multifaceted complications underscore the critical need for research26 research to identify and develop effective therapeutic strategies to accelerate diabetic wound healing and prevent severe outcomes (2–5).

Current treatment strategies available for diabetic wound healing include keeping the wound slightly moist, applying topical gel or antibiotic ointment medication, debridement, and monitoring blood sugar levels. However, these treatments have some disadvantages (6). Keeping the wound moist can increase the risk of infection if the wound becomes too wet. Topical gel or antibiotic ointment medication can cause allergic reactions in some people. Debridement can be painful and may require anaesthesia. Monitoring blood sugar levels can be challenging and requires frequent testing. Additionally, current treatments do not guarantee a rapid and definite reparative process, making diabetic wounds a challenge to treat. Therefore, there is a need for therapeutic alternatives to the currently available treatments.(7)

Diabetic wounds are a multifaceted problem that requires a multifaceted approach to treatment. The pathophysiology of diabetic wounds is complex, involving deregulated angiogenesis, chronically sustained sub-optimal inflammatory response, increased levels of reactive oxygen species, and persistent bacterial colonization that often develops into a hard-to-treat biofilm. Therefore, current and upcoming diagnostic and treatment strategies for diabetic wounds are

diverse and multifunctional. A multifaceted approach is necessary to address the various factors that contribute to diabetic wound healing, including impaired circulation, neuropathy, and infection (8,9).

Boswellia acid, a resin extract from the Boswellia tree, has been found to have potential in the treatment of diabetic wounds. Studies have shown that Boswellia cream 2.5% increased the rate of epithelial tissue and collagen fibre synthesis and wound healing in rats with diabetic wounds(10). The standardized extract of Boswellia serrata has also been found to have wound healing potential and possible mechanisms of action against experimental models of diabetic foot ulcers. Histopathologic studies have shown that the rate of epithelial tissue and collagen formation, as well as wound healing, was higher in the group treated with Boswellia serrata(11). Boswellia acid has antimicrobial, antioxidant, anti-inflammatory, and analgesic properties, making it widely used for skin disorders, rheumatism, and central nervous system diseases (12).

Quercetin, a natural flavonoid abundantly found in various fruits, vegetables, and herbs, has gained significant attention for its potential role in diabetic wound healing (13). Diabetes mellitus is associated with impaired wound healing due to various factors, including oxidative stress, inflammation, and compromised microcirculation (14). Quercetin's antioxidant properties make it a compelling candidate for mitigating oxidative stress and reducing inflammation, both of which are key contributors to delayed wound healing in diabetes. Its ability to scavenge free radicals and modulate inflammatory pathways can help create a conductive environment for tissue repair(15).

Quercetin also exhibits antimicrobial properties, which are essential in preventing and controlling wound infections, particularly in diabetic patients who are susceptible to infections due to compromised immune function(16). By inhibiting the growth of bacteria and other pathogens, quercetin can help maintain a sterile environment that promotes healing (17).

Furthermore, studies have shown that quercetin promotes diabetic wound healing by switching macrophages from M1 to M2 polarization, thereby inhibiting inflammatory reactions (18,19).

2. Materials and methods

2.1. Materials

Boswellic acid extract (30% purity) was obtained from Shivatava Enterprises in Aurangabad, India. Quercetin hydrate was purchased from New Neeta Chemicals in Pune, India. Carbopol 934, triethanolamine, sodium metabisulfite, sodium benzoate, nutritious agar (1.5% agar), agar-agar media, and glycerin were obtained from Loba Chemie Pvt. Ltd. in Mumbai. The solvents and chemicals employed in this study were of analytical grade.

2.2. Method

2.2.1. Pre-formulation

Foam degradation test:

To quantify the extent of degradation, initial dry dressing samples were weighed and designated as W_0. The samples were then fully immersed in 7 mL of phosphate-buffered saline (PBS, pH 7.4) within a 6-well plate and incubated at a constant temperature of 37°C. The PBS was

replaced daily to maintain an optimal environment for the samples. After a 48-hour incubation period, the samples were carefully removed from the PBS and rinsed with distilled water to remove residual buffer solution. The rinsed samples were dried at 40°C for an additional 48 hours to ensure complete moisture removal, achieving a final dry state. The dried samples were then reweighed and recorded as W_1, representing their final dry weight post-degradation. The extent of degradation was determined by comparing the initial dry weight (W_0) with the final dry weight (W_1) (20).

$$\text{Percent degradation} = \frac{(W0 - W1)100}{W0}$$

Absorbency:

To check how well the dressings absorb, 5 cm by 5 cm samples were made. A test solution, called Solution A, was created by mixing 0.368 grams of calcium chloride dihydrate and 2.298 grams of sodium chloride into 1 litre of deionized water. Each dressing sample was weighed and put into its own Petri dish. Solution A was warmed to 37 degrees Celsius, and a volume equal to 40 times the weight of each sample was carefully added to the dressings. The dishes were kept at a steady 37 degrees Celsius for 30 minutes. After that, the dishes were taken out, and each sample was lifted by one corner for 30 seconds to let the extra liquid drip off. Then, the samples were weighed again to find out how absorbent the dressings were. (21).

$$Mass\ loss\ upon\ drying\ (\%) = \frac{B - A \times 100}{B}$$

Where, A= mass of specimens after testing, B mass of specimens before testing.

Dehydration rate of dressing:

The dehydration behaviour was assessed by calculating the disparity in mass between the wet and dry specimens. Initially, the specimens were subjected to a 24-hour drying period within an incubator set at a temperature of 37±1°C to attain their completely dry state. The mass of these dry specimens was recorded before immersing them in an excess volume of solution (prepared by dissolving 0.368g of calcium chloride dihydrate and 2.298g of sodium chloride in 1 litre of de-ionized water), also maintained at 37±1°C, for 30 minutes. Following this immersion, the specimens were carefully extracted from the fluid and suspended by one corner to facilitate free drainage for 30 seconds. Subsequently, they were reweighed and transferred into Petri dishes, where they were placed in an incubator. The dehydration behaviour of the specimens was quantified by calculating the mass difference between their wet and dry states. Initially, specimens were dried in an incubator at 37 ± 1°C for 24 hours to reach a fully desiccated state, and their dry masses were recorded. The dried specimens were then submerged in an excess volume of a test solution, prepared by dissolving 0.368 g of calcium chloride dihydrate and 2.298 g of sodium chloride in 1 L of deionized water, maintained at 37 ± 1°C, for 30 minutes. Post-immersion, the specimens were carefully extracted, suspended by one corner to allow excess solution to drain freely for 30 seconds, and reweighed to determine their wet mass. Subsequently, the specimens were transferred to Petri dishes and returned to the incubator at 37 ± 1°C for an additional 24 hours to assess further dehydration. The rate of dehydration was measured in grams per minute (g/min)(22).

$$Dehydration\ rate = \frac{(W - D)}{T}$$

Where, W = Wet mass of specimens,
D = Dry mass of specimens,
T = Test period in minutes

Rate of absorption

To assess the absorption rate, a test solution, prepared by dissolving 0.368 g of calcium chloride dihydrate and 2.298 g of sodium chloride in 1 L of deionized water, was applied dropwise to the wound contact layer surface of each dressing using a calibrated eye dropper. The time required for complete absorption of each drop was recorded in seconds. A total of 20 drops were applied to each dressing, and the mean absorption time was calculated for each specimen(23,24).

2.2.2. Formulation of wound healing gel

Fresh aloe vera leaves were used to extract aloe vera juice, which was then mixed with an equal amount of deionized water and ethanol in a 1:1:1 ratio. Carbopol 934 was hydrated in the diluted aloe vera juice for 24 hours to form a gel base. Subsequently, sodium metabisulfite, sodium benzoate, and glycerine were incorporated into the gel and stirred continuously for 1 hour to ensure homogeneity. Quercetin hydrate and boswellic acid extract (30% purity) were then added, and the mixture was stirred for an additional 30 minutes. The pH of the resulting formulation was adjusted to 6.4 using triethanolamine(25,25). Composition of wound healing gel given in Table 1.

2.2.3. Loading of wound healing gel into polyurethane foam

Polyurethane foam samples were sterilised using gaseous sterilisation. Five square pieces of polyurethane foam, each measuring 1 inch × 1 inch, were placed on a Petri dish. A 0.5 g aliquot of the prepared gel was uniformly applied to the top surface of each foam piece. The samples were incubated for 24 hours to allow complete absorption of the gel by the foam (26).

Table 1: Composition of wound-healing gel

Ingredients	Quantity
Aloe Vera gel	20%
Carbopol 934	1.5%
Sodium metabisulphite	1.5%
Sodium benzoate	1%
Boswellia extract	2.5%
Quercetin	1%
Triethanolamine	q.s to adjust pH to 6.8
Glycerin	1%
Purified water	q.s. up to 100 gm

2.2.4. Evaluation of wound healing gel

Viscosity

Viscosity measurements were performed using a DV-II+ Pro Brookfield viscometer equipped with spindle no. 93, operated at a rotational speed of 0.5 rpm and maintained at a constant temperature of 37°C (27).

Spreadability

The spreadability was assessed using a CT3 texture analyzer equipped with a 1000-gram load cell and a stability base table. The test was conducted in compression mode using male and female conical probes. The speed of pre-testing, testing and testing was set to 2 mm/s. The target parameter was the distance, with a target value of 4 mm, and the trigger force was set to 10 grams. The female conical probe was filled with samples, and the surface was levelled using a flat knife. Load cell -linked male conical check, aligned with female probe for testing (28).

Antioxidant Assays

The antioxidant capacity of ascorbic acid (control) and the wound healing dressing was assessed using the 2,2-diphenyl-1-picrylhydrazyl (DPPH) assay. Methanolic DPPH solution was added to the wound healing gel samples. The mixtures were vigorously vortexed and incubated at room temperature in the dark for 30 minutes to ensure complete reaction. The absorbance of each sample was measured at 517 nm using a spectrophotometer. The percentage antioxidant activity was calculated using the following equation.

$$\%\ \text{Antioxidant activity} = \frac{(\ \text{absorbance of control} - \text{absorbance of sample}) \times 100}{\text{absorbance of control}}$$

2.2.5. Evaluation of dressing system

pH

The pH of the dressing was measured using a calibrated pH meter.

Skin irritation test

In vitro dissolving studies were conducted using a USP type I (basket) mechanism. Foam dressing, each in 40 mg Boswellia extract, quercetin and aloe vera gel, was placed in individual disintegration ships. The use was used at a controlled temperature of 37 ° 1 °C with a basket rotation speed of 100 rpm. The dissolution medium included a phosphate buffer solution (pH 6.8) and 900 mL of methanol mixture in the ratio of 80:20. At a predetermined time interval (30, 60, 90, 120, 150, and 180 minutes), 5 mL samples were withdrawn through disintegration, and a similar amount of fresh phosphate buffer solution (pH 6.8) was added to maintain the position of the sink. The study was conducted over 3 hours. The absorption of withdrawn samples was measured at 369 nm and 250 nm (29,30).

Antibacterial activity

Ex vivo antibacterial activity

The ex vivo antibacterial activity of the test compound was evaluated against Pseudomonas aeruginosa, Bacillus subtilis, Bacillus cereus, Bacillus coagulans, Escherichia coli, and Staphylococcus aureus using the agar well diffusion method. Bacterial cultures were propagated on nutrient agar slants and subsequently suspended in nutrient broth for overnight incubation at 37°C. A volume of 100 µL of the bacterial suspension was uniformly spread onto Mueller-Hinton agar plates. Wells were created in the agar using a sterile cork borer, and the test gel was introduced into the wells. The plates were incubated at 37°C for 24 hours. Antibacterial activity was assessed by measuring the diameter of the clear zone of inhibition

surrounding each well, expressed in millimetres.(31,32)

In-Vivo study

Approval of protocol

All experimental procedures and protocols employed in this study were reviewed and approved by the Institutional Animal Ethical Committee (IAEC) of AISSMS College of Pharmacy (Approval No. CPCSEA/IAEC/PT-20/01-2K20). Experiments were conducted in strict accordance with the ethical guidelines established by the Committee for Control and Supervision of Experiments on Animals (CPCSEA).

Animals

Wistar rats, weighing 150–170 g, were randomly assigned to four experimental groups. The animals were housed in stainless steel cages and provided with a standard commercial laboratory rat diet. All rats remained conscious throughout the duration of the study.

Skin irritation test

A skin irritance test was performed using a rat model. The dorsal skin of the rats was shaved, and methylated spirit was applied to the shaved area as an antibacterial agent. The foam dressing was applied to the shaved skin of the test group. After application, skin sites were observed daily for three days. The primary dermal irritation index (PDII) was used to evaluate skin irritation, with a PDII score of 0 indicating that there is no irritation and a score greater than 5.0 indicating severe irritation(21,33,34).

Excision wound model

An anisotropies lesion model was installed in mice under Ether anaesthesia. The dorsal area of mice was shaved, and a full-thickness wound was made on the back using a scalpel and sharp scissors. The wound site was sterilized with ethanol, and a portion of the skin was extracted from the marked area, resulting in the wound measuring about 2.5 cm in length and 0.2 cm in depth. Until the haemorrhage was completely controlled, hemostasis was achieved by applying a warm saline-lact cotton swab to the wound. Post-proseder, each rat was personally placed in a cage. Treatment was started on the day of construction of the wound, either with a standard emollient (marketing povidone-iodine ointment) or the application of an experimental testing point. To cover the surface of the wound, both yogas were gently applied and continued daily until the entire wound stopped, and therapy was observed. The wound diameter was measured daily using a transparent ruler until the full bandh was obtained. To assess the efficacy of treatment in wound healing and promoting tissue regeneration, the wound healing activity was evaluated based on the wound contraction rate, expressed as one per cent. Regular measurement provided comprehensive data on the progress of wound healing during the study period (35,36). The treatment groups are given in Table 2.

Table 2: Treatment groups

Groups	Group: 1	Group: 2	Group: 3	Group: 4
Animal (n=6)	Normal control	Diabetic control	Standard group	Test group
Treatment	No treatment	No treatment	Povidone Iodine Ointment	Test foam dressing

The following formula was used to calculate the percentage wound contraction:

$$\%\ Wound\ contraction = \frac{(\text{Wound area on day zero} - \text{Wound area on day n}) \times 100}{\text{Wound area on day zero}}$$

Estimation of Hydroxyproline and Hexosamine:

On days 4, 8, and 16 post-surgical excision, skin tissue samples were collected from the healed wound site for hydroxyproline content analysis, a key indicator of collagen presence. The tissues were dried to a constant weight in a hot air oven maintained at 60–70°C. The dried samples were hydrolyzed in 6 N hydrochloric acid (HCl) at 130°C for 4 hours in sealed tubes. The hydrolysate was neutralized to pH 7.0, followed by oxidation with Chloramine T for 20 minutes. The reaction was terminated by adding 0.4 M perchloric acid, and colour development was achieved using Ehrlich's reagent at 60°C. Absorbance was measured at 557 nm using a UV/Vis spectrophotometer (Shimadzu, Japan).

Granulation tissues were weighed and hydrolyzed in 6 N HCl at 98°C for 8 hours to determine hexosamine content. The hydrolysate was neutralized to pH 7.0 with 4 N sodium hydroxide (NaOH) and diluted with Milli-Q water. The hexosamine content was quantified with modifications to established protocols. The diluted solution was combined with acetyl acetone solution and heated at 96°C for 40 minutes. After cooling, 96% ethanol and p-dimethylamine-benzaldehyde solution (Ehrlich's reagent) were added, and the mixture was thoroughly mixed and incubated at room temperature for 1 hour. Absorbance was measured at 530 nm using a double-beam UV/Vis spectrophotometer (Shimadzu, Japan). Hexosamine content was calculated by comparison with a standard curve and expressed as milligrams per gram of dry tissue weight.

Histological examination:

Tissue samples from the wound site were fixed in 10% phosphate-buffered formalin, dehydrated through a graded ethanol series, and embedded in paraffin. Sections of 4–5 µm thickness were prepared using a microtome and stained with haematoxylin-eosin (H&E) and Masson's trichrome to evaluate tissue morphology and collagen content, respectively. Photomicrographs were captured using a light microscope (model unspecified) for detailed histological assessment.

The following parameters were evaluated: fibroplasia, collagen deposition, neovascularisation, leukocyte infiltration, skin appendage regeneration, epidermal re-epithelialization, and overall wound healing grade. Each parameter was scored on a scale of 0–4, defined as follows: 0 = no closure; 1 = <30% closure; 2 = 31–60% closure; 3 = 61–99% closure; 4 = complete re-epithelialization by keratinocytes. The extent of each parameter was further graded qualitatively from minimal (1/+) to marked (4/++++).

3. Result

3.1. Preformulation studies of foam

Degradation test

The objective of this study was to evaluate the degradation profile of a foam dressing material under conditions mimicking physiological environments. The foam was immersed in a phosphate buffer solution (pH 7.4) for 48 hours to simulate exposure to bodily fluids. As presented in Table 3, the foam exhibited minimal weight loss, with a degradation rate of approximately 0.56%. This negligible mass reduction indicates exceptional resistance to deterioration under the tested conditions.

The observed stability underscores the foam's ability to maintain structural integrity and physical properties when subjected to potential degradative factors. These findings highlight the material's suitability for applications requiring robust performance, such as wound management, where durability and reliability are paramount. The foam's capacity to remain intact over a 48-hour incubation period in a simulated physiological environment supports its potential efficacy and dependability for clinical use.

Table 3 Percentage foam degradation

Initial weight of PU foam (gm)	Weight after foam degradation test (gm)	Percentage degradation
0.351	0.349	0.56±0.05%
		n=3

Absorbency

The polyurethane foam dressing demonstrated a remarkable absorption capacity, retaining approximately four times its dry mass per unit area of the test solution. Peak absorption reached 18 g/g, indicating high fluid uptake efficiency. However, this enhanced absorption was associated with a 20% mass loss, suggesting potential structural degradation or material dissolution during fluid interaction. Notably, no direct correlation was observed between absorption behaviour and the dressing’s mass or thickness, indicating that other intrinsic material properties may govern fluid uptake.

Upon application of the solution, the dressing exhibited complete swelling, with each layer expanding uniformly. This swelling behaviour is hypothesized to enhance wound healing by facilitating ventilation and supporting moisture balance at the wound site. The collaborative contribution of individual layers underscores the dressing’s potential to optimize the wound recovery process.

Dehydration rate

The dehydration rate of the polyurethane foam dressing was determined to be 0.024 g/min. An inverse relationship was observed between dressing thickness and dehydration rate, where the

fraction of water released at a given time decreased as the thickness of the dressing increased. This suggests that thicker dressings retain moisture more effectively over time.

Rate of absorption

The polyurethane foam dressing exhibited a moderate absorption rate, with an average absorption time of 7 seconds for Solution A. This rate indicates efficient fluid uptake suitable for less exuding wounds. The dressing maintained structural integrity and effectively prevented strike-through of the simulated exudate, supporting its design for prolonged application exceeding 6 hours.

3.2. Evaluation of wound healing gel:

Viscosity:

The viscosity of the formulated wound healing gel was measured at 143,000 cps. This high viscosity indicates a thick, semi-solid consistency, which poses potential challenges for uniform incorporation into the porous structure of polyurethane foam dressings. Conversely, the elevated viscosity minimizes the risk of dropping off during application, ensuring stable retention within the dressing.

Spreadability

The hardness of the gel was determined to be 54.16 g, indicative of substantial firmness, which facilitates ease of handling and application. The adhesiveness of the gel was measured at 1.62 mJ, reflecting the strength of interaction between the gel and the application surface or site.

Antioxidant activity:

The antioxidant activity of the gel was determined to be 83%, demonstrating significant potential to neutralize free radicals and mitigate oxidative stress. For comparison, ascorbic acid, employed as a positive control, exhibited an antioxidant activity of 87%. Antioxidant activity is defined as the capacity of a substance to scavenge or neutralize free radicals and reactive oxygen species (ROS) within biological systems. Free radicals, characterized by their high reactivity, can induce cellular damage through electron abstraction from adjacent molecules, thereby contributing to oxidative stress.

3.3. Evaluation Test of dressing

pH:

The pH of the polyurethane foam dressing was determined to range between 6.4 and 6.8. The pH level is a critical factor in diabetic wound healing, as it significantly influences the wound microenvironment. An optimal pH range reduces infection risk by creating conditions less conducive to the proliferation of pathogenic microorganisms. Furthermore, precise pH control mitigates chronic inflammation and supports essential cellular processes integral to tissue repair, including collagen synthesis and angiogenesis. In the context of diabetic wounds, maintaining an appropriate pH balance is necessary for preventing chronic wound development and promoting effective healing.

Skin Adhesion Test

The bio-adhesion strength of the polyurethane foam dressing was quantified as the force required to detach the dressing from a surface following adhesion. The skin adhesion test was

conducted using a CT3 Brookfield Texture Analyser, revealing an adhesiveness value of 0.12 mJ. The observed adhesion strength indicates that the dressing possesses sufficient adhesive properties for effective application.

In vitro Dissolution Study

The percentage cumulative Boswellia extract release of dressing in methanolic phosphate buffer pH 6.8 medium was found to be 99.44% and 51.44% for quercetin (Fig. 1).

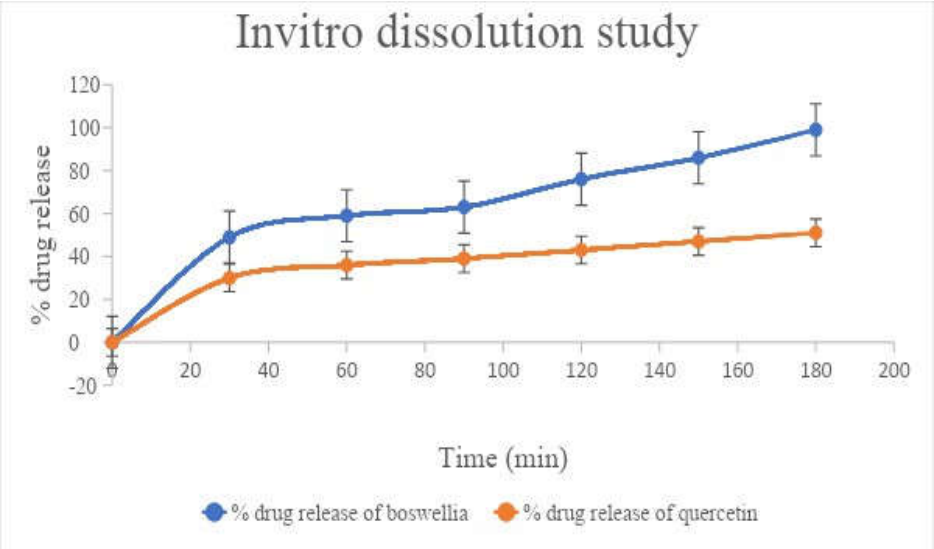

Fig.1: Percentage (%) drug release of dressing

Antibacterial activity

The antibacterial efficacy of the gel formulation was assessed through the measurement of the zone of inhibition for three samples, as presented in Table 4. Diabetic wounds are highly susceptible to bacterial infections, which can significantly impede the healing process and lead to severe complications. Evaluation of the formulation's antibacterial activity is crucial for determining its capacity to prevent and combat infections caused by common pathogens, thereby reducing the risk of wound infection. These studies provide insights into the gel's antibacterial performance in ex vivo conditions, simulating real-world patient scenarios and generating critical data to support regulatory approvals and clinical recommendations. Results from the ex vivo antibacterial activity assays demonstrate that the wound dressing effectively inhibits the growth of *Pseudomonas aeruginosa*, *Bacillus subtilis*, *Bacillus cereus*, *Bacillus coagulans*, *Escherichia coli*, and *Staphylococcus aureus*. These findings indicate that the gel serves as a potent treatment option for managing wound infections caused by these bacterial pathogens.

Table 4: Ex vivo antibacterial activity of formulation

Sample	Zone of Inhibition (mm)					
	S. aureus	E. coli	Pseudomonas aeruginosa	Bacillusubtili	Bacillus cereus	Bacillus coagulans

Wound healing dressing	13.6±1	15 ±1	14.1±1	11.3±1	12.6±1	14.6±1
Negative control (Dimethyl sulfoxide	4±1	3±1	5±1	3±1	6±1	2±1
Positive control (Streptomycin)	29.6±1	31.6±1	29±1	28 ±1	27±1	26±1

Skin Irritation Test

The primary dermal irritation index (PDII) for the wound dressing was determined to be 0, indicating an absence of erythema, oedema, or other signs of irritation on the rat skin model. These findings demonstrate that the formulation is non-irritating and safe for topical application.

In-Vivo Study

The test group was treated with a developed foam dressing. The standard group was treated with povidone-iodine ointment, and the control group remained undressed; the diabetic control group also remained undressed.

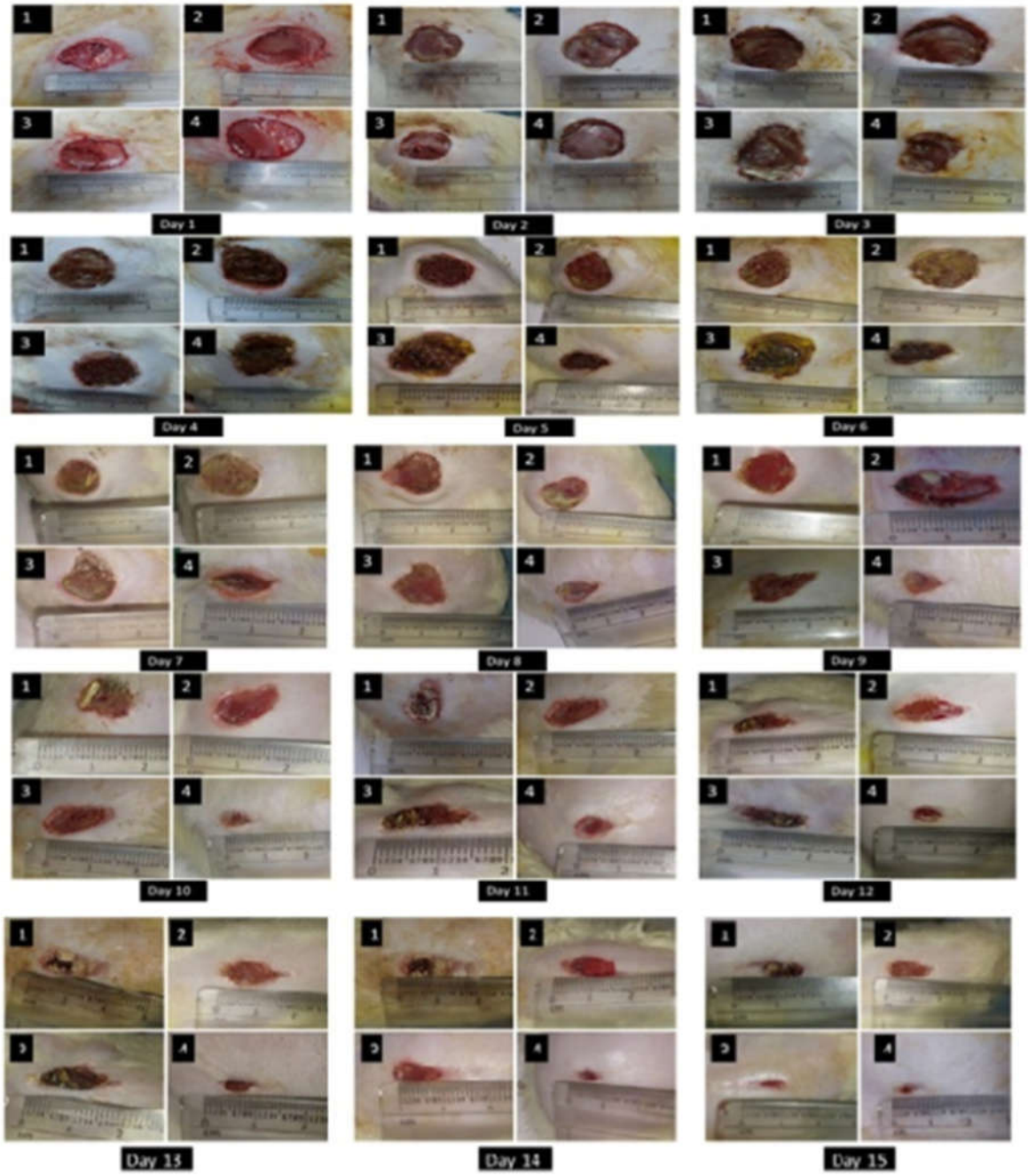

Fig.2: Wound contraction on days 1,3,5,8,11, and

Table 5: Wound area and percentage of wound closure at 0,5,8 and 15 days.

Day	Wound parameter	Normal control	Diabetic control	Standard	Test
0	Wound area % wound closure	297±0.012 0.0	338±0.14 0.0	296±0.06 0.0	266±0.17 0.0
5	Wound area % wound closure	277.7±2.71 6.5±1.5	321.1±3.67 5±1.3	262.56±9.74 11.3±1.8	135.93±2.78 48.9±1.32
8	Wound area % wound closure	246.51±4.16 17±2.0	300.49±2.36 11.1±1.64	233.55±4.02 21.1±1.36	63.84±3.45 76±2.01
15	Wound area % wound closure	187.11±4.36 37±1.87	292.04±1.34 13.6±0.58	211.94±3.24 28.4±1.54	5.32±2.14 98±1.67

Table 5 and Figure 2 illustrate the percentage of wound closure at designated time points (days 0, 5, 8, and 15) across four treatment groups: Normal control, Diabetic control, Standard formulation, and Test formulation. These data provide critical insights into the comparative efficacy of the treatments in facilitating wound healing.

At day 0, serving as the baseline, all groups exhibited 0% wound closure, confirming the initial wound creation stage. By day 5, differential progress was observed. The Normal control group achieved 6.5% wound closure, while the Diabetic control group showed a marginally lower closure rate of 5.0%. The Standard formulation group demonstrated enhanced wound closure at 11.3%, suggesting its capacity to promote early-stage wound healing. Notably, the Test formulation group exhibited a significantly higher wound closure rate of 48.9%, indicating superior efficacy in accelerating wound healing during the initial phase.

By day 8, the disparities in wound closure rates among the groups became more pronounced. The Normal control group exhibited 17.0% wound closure, reflecting consistent healing progression. In contrast, the Diabetic control group displayed a reduced closure rate of 11.1%, underscoring the impaired wound healing associated with diabetic conditions. The Standard formulation group maintained its efficacy with 21.1% wound closure, further supporting its positive influence on the healing process. Remarkably, the Test formulation group achieved an exceptional 76.0% wound closure, highlighting its substantial potential to expedite wound healing.

By day 15, significant wound closure was observed across all groups. The Normal control group exhibited 37.0% closure, indicative of the natural progression of wound healing. The Diabetic control group showed 13.6% closure, further underscoring the delayed healing process in diabetic conditions. The Standard formulation group supported wound closure at 28.4%, demonstrating continued efficacy. In contrast, the Test formulation group achieved an outstanding 98.0% wound closure, highlighting its remarkable ability to facilitate rapid and near-complete wound healing.

Estimation of hydroxyproline and hexosamine:

Hydroxyproline serves as a critical biochemical marker for collagen content in tissues, given its integral role as a constituent amino acid in collagen molecules. Quantification of hydroxyproline levels provides an indirect measure of collagen synthesis and deposition within the wound microenvironment. During the initial phases of wound healing, hydroxyproline content is typically reduced, reflecting the early stages of collagen biosynthesis. As the healing process advances, an increase in hydroxyproline levels corresponds to the formation of mature collagen fibres, facilitating wound closure and tissue remodelling. Temporal analysis of hydroxyproline concentrations serves as a reliable indicator of the efficacy of therapeutic interventions in promoting collagen synthesis and accelerating wound repair. Monitoring these changes enables a quantitative assessment of treatment outcomes in the context of tissue regeneration and extracellular matrix maturation.

Table 6 presents the hydroxyproline content in wound tissue across different experimental groups at multiple time points, providing insights into the dynamics of collagen synthesis and tissue regeneration during wound healing. On day 4, hydroxyproline levels, indicative of early collagen deposition, varied significantly among groups. The normal control group recorded a

hydroxyproline content of 3.1 ± 0.16 µg/mg, reflecting baseline collagen synthesis. The standard formulation group exhibited a higher content of 3.8 ± 0.22 µg/mg, while the test formulation group demonstrated the highest level at 8.8 ± 0.22 µg/mg, suggesting enhanced collagen production.

By day 8, collagen deposition progressed across all groups. The normal control group showed an increase to 6.1 ± 0.54 µg/mg, and the standard formulation group reached 6.4 ± 1.2 µg/mg. The test formulation group maintained its superior performance with a hydroxyproline content of 12.6 ± 1.2 µg/mg, underscoring its pronounced effect on collagen synthesis. On day 15, collagen accumulation continued, with the normal control group exhibiting 7.9 ± 0.21 µg/mg and the standard formulation group reaching 8.2 ± 0.89 µg/mg. The test formulation group sustained its elevated hydroxyproline content at 17.2 ± 0.89 µg/mg, highlighting its consistent and robust promotion of collagen formation throughout the healing process.

These hydroxyproline estimation results elucidate the differential effects of the tested formulations on collagen synthesis, a pivotal process in wound repair. The test formulation consistently demonstrated the highest hydroxyproline levels across all time points, indicating its superior capacity to enhance collagen production and extracellular matrix maturation. This aligns with observed wound closure rates, suggesting that the test formulation significantly accelerates wound healing compared to the standard and control groups.

Table 6: Estimation of hydroxyproline

Group Name	Day 4	Day 8	Day 15
Normal control	3.1±0.16	6.1±0.54	7.9±0.21
Standard formulation	3.8±0.22	6.4±1.2	8.2±0.89
Test formulation	8.8±0.22	12.6±1.2	17.2±0.89

n=3

The quantification of hexosamine content is a critical parameter in elucidating the molecular mechanisms underlying wound healing. Hexosamines, integral constituents of glycoproteins, proteoglycans, and other complex carbohydrates, are essential for tissue regeneration and extracellular matrix (ECM) formation. The assessment of hexosamine levels provides valuable insights into the biochemical processes driving wound repair. These compounds are intricately involved in key biological functions, including cell adhesion, migration, proliferation, and the synthesis of ECM components, all of which are indispensable for effective wound healing and tissue restoration.

Glycosaminoglycans (GAGs), which incorporate hexosamines as key structural units, are fundamental components of the extracellular matrix (ECM), contributing to tissue integrity, hydration, and molecular signalling. Variations in hexosamine content serve as indicators of altered GAG synthesis, which significantly influences cellular behaviour and tissue architecture during wound healing. These changes modulate critical processes such as cell migration, proliferation, and ECM remodelling, thereby playing a pivotal role in the orchestration of tissue repair and regeneration.

The hexosamine content across different experimental groups at various time points is summarised in Table 7. These findings provide critical insights into the dynamics of wound healing and the effects of distinct formulations on hexosamine levels. The observed variations

in hexosamine content reflect alterations in the synthesis of glycoproteins, proteoglycans, and other carbohydrate-rich macromolecules, which are essential for tissue regeneration and extracellular matrix formation during the wound repair process.

On day 4, variations in hexosamine content were observed across the experimental groups. The normal control group exhibited a hexosamine level of 0.04 µg/mg, representing the baseline concentration of these essential compounds during the early phase of wound healing. In contrast, the standard formulation and test formulation groups demonstrated modest elevations in hexosamine content, with values of 0.05 µg/mg and 0.06 µg/mg, respectively. These findings suggest that both the standard and test formulations may have mildly stimulated hexosamine synthesis, potentially enhancing the production of glycoproteins and proteoglycans critical for tissue repair.

By day 8 of the wound healing process, distinct differences in hexosamine content were observed among the experimental groups. The normal control group maintained a hexosamine level of 0.05 µg/mg, while the standard formulation group showed a slight increase to 0.06 µg/mg. In contrast, Test Formulation 1 demonstrated a significant elevation in hexosamine content, reaching 0.16 µg/mg. This marked increase suggests a substantial enhancement of hexosamine synthesis, likely indicative of augmented glycoprotein and proteoglycan production. These findings point to a favourable tissue regeneration environment promoted by Test Formulation 1, highlighting its potential efficacy in supporting wound repair.

On day 15 of the wound healing process, hexosamine content continued to demonstrate progressive changes across the experimental groups. The normal control group exhibited a hexosamine level of 0.06 µg/mg, reflecting a gradual increase over the healing period. Similarly, the standard formulation group showed a modest rise to 0.07 µg/mg. Notably, Test Formulation 1 sustained its pronounced effect, with a hexosamine content of 0.23 µg/mg, indicating a persistent enhancement of hexosamine synthesis. This sustained elevation suggests that Test Formulation 1 significantly promotes the production of glycoproteins and proteoglycans, thereby fostering an optimal environment for tissue regeneration throughout the later stages of wound healing.

Table 7: Estimation of hexosamine

Group Name	Day 4	Day 8	Day 15
Normal control	0.04±0.0	0.05±0.0	0.06±0.0
Standard formulation	0.05±0.0	0.06±0.0	0.07±0.0
Test formulation	0.06±0.0	0.16±0.0	0.23±0.0

n=3

Histological examination

Table 8: Observations of histopathological studies

Histopathological parameters	8 days	15 days
Fibroplasia	Mild to moderate effect on the dermal bridging of wound edges	Profound and adequate to effect complete dermal bridging
Laid down Collagen	Not seen	Mild to moderate

Average Neovascularization	Mild (4 to 7/hpf)	Moderate (8 to 11/hpf)
Leucocytic infiltration	Profound; neutrophilic in the superficial necrotic area; deeper tissue showed lymphocytes & macrophages	Minimal lymphocytic infiltration in the deeper parts of the granulation tissue
Regeneration of skin appendages	Not seen	Not seen
Epidermal repair	Absent. Only scab formation. The scab was not firmly adhered to the underlying necrotic surface of granulation tissue.	97% length is covered with complete epidermal layers.
Grade of healing	Moderate	Profound

Histopathological analysis of wound tissue at two critical time points, days 8 and 15 post-injury, provides comprehensive insights into the dynamic progression of wound healing. On day 8, examination revealed mild fibroplasia, indicative of the initial formation of tissue bridging, with no evidence of collagen deposition, suggesting that collagen synthesis had not yet commenced. Neovascularisation was observed at a minimal level, reflecting early angiogenesis to facilitate nutrient and oxygen delivery to the wound site. A pronounced leukocytic infiltration, predominantly composed of neutrophils, with contributions from lymphocytes and macrophages, highlighted an active inflammatory response focused on debris clearance and initiation of the healing cascade. Notably, no regeneration of skin appendages was observed at either time point. Epidermal repair was absent on day 8, with only a loosely adhered scab present. By day 15, significant progress was evident, with nearly complete epidermal coverage across the wound length. Overall, the wound healing process demonstrated moderate advancement on day 8 but exhibited substantial improvement by day 15, achieving a high healing grade. This transition reflects a shift from early inflammatory and tissue initiation phases to advanced stages characterized by enhanced tissue regeneration, collagen deposition, and significant epidermal repair, as summarised in Table 8 and illustrated in Figure 3.

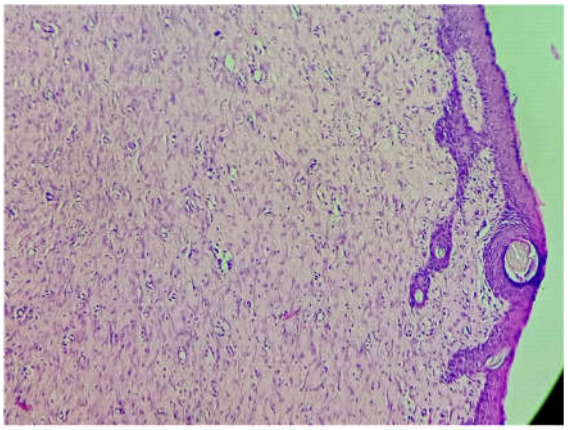

Day 8

Day 15

Figure 3: Histopathological images obtained on days 8 and 15

4. Discussion:

The polyurethane foam (PUF) exhibited exceptional stability during degradation testing. Exposure to a phosphate buffer solution (pH 7.4) for 48 hours resulted in minimal weight loss of approximately 0.56%, indicating robust structural integrity under conditions mimicking physiological fluids. This durability is a critical attribute for wound dressings, ensuring sustained performance in clinical applications.

The PUF demonstrated superior absorbent capacity, absorbing approximately four times its dry mass per unit area in solution. This high absorbency is attributed to the open-cell structure of the foam, which facilitates substantial fluid retention. Such properties are essential for maintaining a moist wound environment conducive to healing. In the dehydration rate test, PUF samples efficiently drained excess solution within 30 seconds, highlighting effective exudate management. Subsequent drying returned the foam to its original state, underscoring its suitability for continuous wound care. The rapid absorption rate was further evidenced by the foam's ability to uptake solution droplets within seconds, enhancing its capacity to manage wound exudate efficiently.

A novel wound healing gel, incorporating Boswellia extract, Quercetin, and Aloe vera, was integrated into the PUF matrix to create a synergistic wound dressing system. Boswellia extract provides anti-inflammatory effects, mitigating inflammation in diabetic wounds. Quercetin, an antioxidant, promotes collagen synthesis and angiogenesis, while Aloe vera supports tissue repair and wound hygiene. The gel exhibited optimal viscosity and spreadability, ensuring uniform application and ease of use in clinical settings. Additionally, the gel demonstrated significant antioxidant activity, crucial for counteracting oxidative stress that impedes wound repair. The pH of the dressing was optimized to align with the physiological range, fostering an environment supportive of natural healing processes.

In vivo studies evaluated the efficacy of the developed wound dressing in promoting incision wound healing in a diabetic model. The dressing significantly accelerated wound closure compared to the normal control, diabetic control, and standard treatment groups, highlighting its potential for clinical application.

Hydroxyproline and hexosamine assays quantified collagen and extracellular matrix (ECM) components in wound tissue. Elevated levels of these markers in the test formulation group indicated enhanced collagen synthesis and ECM formation, supporting the dressing's role in promoting tissue regeneration dynamics.

On day 8, mild fibroplasia and minimal collagen deposition were observed, reflecting delayed collagen synthesis typical in diabetic wounds. Mild neovascularisation indicated limited angiogenesis, underscoring the need for enhanced blood supply to improve nutrient and oxygen delivery. Robust leukocytic infiltration, primarily neutrophilic with contributions from lymphocytes and macrophages, signified an active inflammatory response on day 8, transitioning to a proliferative phase by day 15. The absence of skin appendage regeneration and delayed epidermal repair highlighted a predominant focus on dermal repair. By day 15, significant progress was evident, with a marked transition from moderate to profound healing, characterized by enhanced collagen deposition, angiogenesis, and re-epithelialization. These findings emphasize the importance of targeting collagen synthesis, neovascularisation, and epidermal repair while managing inflammation and pH in diabetic wound care strategies.

5. Conclusion

The thorough evaluation of the wound dressing system, encompassing its absorbency, degradation, and the integration of a bioactive wound healing gel, underscores its efficacy as an advanced therapeutic strategy for diabetic wound care. By combining a highly absorbent and robust polyurethane foam with a bioactive gel, this innovative system provides a comprehensive approach to tackling the multifaceted challenges of diabetic wound management, as evidenced by its promising in vitro and in vivo performance.

6. DECLARATION

Consent for publication

Not applicable

Availability of data and materials

The datasets used and/or analysed during the current study are available from the corresponding author on reasonable request.

Competing interests

The authors declare that they have no competing interests.

Funding

All study protocol is self-funded by authors.

Authors contributions

RP confirmed entire study protocol and major contributor in performing evaluation studies. AM supervised research work. SD studied, performed in vitro studies and major contributor in manuscript writing. Others are for resources and investigation.

7. References

1. The pathophysiology of diabetic foot: a narrative review [Internet]. [cited 2025 Aug 16]. Available from: https://www.e-jyms.org/journal/view.php?number=2810
2. Wound healing - A literature review - PubMed [Internet]. [cited 2025 Aug 16]. Available from: https://pubmed.ncbi.nlm.nih.gov/27828635/
3. Burgess JL, Wyant WA, Abdo Abujamra B, Kirsner RS, Jozic I. Diabetic Wound-Healing Science. Medicina (Mex). 2021 Oct 8;57(10):1072.
4. He J, Chen J, Liu T, Qin F, Wei W. Research Progress of Multifunctional Hydrogels in Promoting Wound Healing of Diabetes. Int J Nanomedicine. 2025 Jun 16;20:7549–78.
5. The Problem of Wound Healing in Diabetes—From Molecular Pathways to the Design of an Animal Model [Internet]. [cited 2025 Aug 16]. Available from: https://www.mdpi.com/1422-0067/23/14/7930
6. Kavitha KV, Tiwari S, Purandare VB, Khedkar S, Bhosale SS, Unnikrishnan AG. Choice of wound care in diabetic foot ulcer: A practical approach. World J Diabetes. 2014 Aug 15;5(4):546–56.
7. Wound Debridement - StatPearls - NCBI Bookshelf [Internet]. [cited 2025 Aug 16]. Available from: https://www.ncbi.nlm.nih.gov/books/NBK507882/
8. Pastar I, Balukoff NC, Marjanovic J, Chen VY, Stone RC, Tomic-Canic M. Molecular Pathophysiology of Chronic Wounds: Current State and Future Directions. Cold Spring Harb Perspect Biol. 2023 Apr;15(4):a041243.
9. Xue Y, Zhou J, Lu Y, Zhang H, Chen B, Dong S, et al. Advancements in Wound Management: Microenvironment-Sensitive Bioactive Dressings with On-Demand Regulations for Diabetic Wounds. Engineering. 2025 May 1;48:234–61.
10. Pengzong Z, Yuanmin L, Xiaoming X, Shang D, Wei X, Zhigang L, et al. Wound Healing Potential of the Standardized Extract of Boswellia serrata on Experimental Diabetic Foot Ulcer via Inhibition of Inflammatory, Angiogenetic and Apoptotic Markers. Planta Med. 2019 May;85(8):657–69.
11. Dong F, Zheng L, Zhang X. Alpha-boswellic acid accelerates acute wound healing via NF-κB signaling pathway. PLOS ONE. 2024 Sep 3;19(9):e0308028.
12. Roy NK, Parama D, Banik K, Bordoloi D, Devi AK, Thakur KK, et al. An Update on Pharmacological Potential of Boswellic Acids against Chronic Diseases. Int J Mol Sci. 2019 Aug 22;20(17):4101.
13. Aghababaei F, Hadidi M. Recent Advances in Potential Health Benefits of Quercetin. Pharmaceuticals. 2023 Jul 18;16(7):1020.

14. Patel S, Srivastava S, Singh MR, Singh D. Mechanistic insight into diabetic wounds: Pathogenesis, molecular targets and treatment strategies to pace wound healing. Biomed Pharmacother. 2019 Apr 1;112:108615.
15. Wang Y, Wei X, Wang L, Qian Z, Liu H, Fan Y. Quercetin-based composite hydrogel promotes muscle tissue regeneration through macrophage polarization and oxidative stress attenuation. Compos Part B Eng. 2022 Dec 1;247:110311.
16. Nguyen TLA, Bhattacharya D. Antimicrobial Activity of Quercetin: An Approach to Its Mechanistic Principle. Molecules. 2022 Apr 12;27(8):2494.
17. Zhu T, Han M, Gu X, Liang Y, Zhu C, Zhou Z, et al. The effects of quercetin and taxifolin on gut microbes, digestion enzymes, antioxidant and inflammatory-related gene expression in the Chinese sucker (*Myxocyprinus asiaticus*). Aquac Rep. 2024 Apr 1;35:102011.
18. Fu J, Huang J, Lin M, Xie T, You T. Quercetin Promotes Diabetic Wound Healing via Switching Macrophages From M1 to M2 Polarization. J Surg Res. 2020 Feb 1;246:213–23.
19. Wu X, He W, Mu X, Liu Y, Deng J, Liu Y, et al. Macrophage polarization in diabetic wound healing. Burns Trauma. 2022 Dec 29;10:tkac051.
20. Ma L, Yang Y, Chen T, Ma L, Deng Q. Developing an NT3-loaded exosomal biodegradable conductive hydrogel combined with EA for targeted treatment of spinal cord injury. Mater Today Bio. 2025 Aug 1;33:101988.
21. In vitro characterisation and evaluation of different types of wound dressing materials | Request PDF [Internet]. [cited 2025 Aug 16]. Available from: https://www.researchgate.net/publication/291298972_In_vitro_characterisation_and_evaluation_of_different_types_of_wound_dressing_materials
22. Lee SM, Park IK, Kim YS, Kim HJ, Moon H, Mueller S, et al. Superior absorption and retention properties of foam-film silver dressing versus other commercially available silver dressing. Biomater Res. 2016 Aug 6;20:22.
23. Physical, morphological, and wound healing properties of a polyurethane foam-film dressing | Biomaterials Research | Full Text [Internet]. [cited 2025 Aug 16]. Available from: https://biomaterialsres.biomedcentral.com/articles/10.1186/s40824-016-0063-5
24. Biomedical materials for wound dressing: recent advances and applications - RSC Advances (RSC Publishing) DOI:10.1039/D2RA07673J [Internet]. [cited 2025 Aug 16]. Available from: https://pubs.rsc.org/en/content/articlehtml/2023/ra/d2ra07673j
25. Shivprasad M. Formulation study of gel containing Pterocarpus santalinus extract for its antiinflammatory activity. WORLD J Pharm Pharm Sci. 2013 Sep 16;2.

26. Chen X qing, Xiao J bo. RP-HPLC-DAD detrmination of flavonoids: separation of quercetin, luteolin and apigenin in Marchantia Convoluta [Internet]. Iranian Journal of Pharmaceutical Research; 2022 [cited 2025 Aug 16] p. 175–81. Report No.: 4. Available from: https://brieflands.com/articles/ijpr-128242#abstract
27. De Souza KCB, Schapoval EES, Bassani VL. LC determination of flavonoids: separation of quercetin, luteolin and 3-O-methylquercetin in Achyrocline satureioides preparations. J Pharm Biomed Anal. 2002 May 15;28(3–4):771–7.
28. Thapa R, Pandey P, Parat MO, Gurung S, Parekh HS. Phase transforming *in situ* gels for sustained and controlled transmucosal drug delivery via the intravaginal route. Int J Pharm. 2024 Apr 25;655:124054.
29. CRYSTAL ENGINEERING OF QUERCETIN BY LIQUID ASSISTED GRINDING METHOD | Jurnal Teknologi (Sciences & Engineering) [Internet]. [cited 2025 Aug 16]. Available from: https://journals.utm.my/jurnalteknologi/article/view/12639
30. Setyawan D, Oktavia IP, Farizka R, Sari R. Physicochemical characterization and In Vitro dissolution test of quercetin-succinic acid co-crystals prepared using solvent evaporation. Turk J Pharm Sci. 2017 Dec;14(3):280–4.
31. Fayolle K, Girard C, Lasfargues P, Koteich S, Kerros S. Comparison of In Vitro Methods for Assaying the Antibacterial Activity of a Mix of Natural Essential Oils Against Zoonotic Bacteria. Microorganisms. 2025 May 14;13(5):1125.
32. Sanam MUE, Detha AIR, Rohi NK. Detection of antibacterial activity of lactic acid bacteria, isolated from Sumba mare's milk, against Bacillus cereus, Staphylococcus aureus, and Escherichia coli. J Adv Vet Anim Res. 2022 Jan 15;9(1):53–8.
33. (PDF) Evaluation Of Wound Healing Activity Of Ethanolic Extract Of Flower Of Calotropis Charak institute of pharmacy mandleshwar , 2 Charak institute of pharmacy mandleshwar [Internet]. [cited 2025 Aug 16]. Available from: https://www.researchgate.net/publication/380215067_Evaluation_Of_Wound_Healing_Activity_Of_Ethanolic_Extract_Of_Flower_Of_Calotropis_Charak_institute_of_pharmacy_mandleshwar_2_Charak_institute_of_pharmacy_mandleshwar
34. Development of a porcine deep partial thickness burn model | Request PDF [Internet]. [cited 2025 Aug 16]. Available from: https://www.researchgate.net/publication/230862513_Development_of_a_porcine_deep_partial_thickness_burn_model
35. Rowland MB, Moore PE, Bui C, Correll RN. Assessing wound closure in mice using skin-punch biopsy. STAR Protoc. 2023 Mar 17;4(1):101989.

36. Das K. Wound healing potential of aqueous crude extract of Stevia rebaudiana in mice. Rev Bras Farmacogn. 2013 Mar 1;23:351–7.